Preparation of Nanosize Anatase and Rutile TiO2 by Hydrothermal Treatment of Microemulsions and Their Activity for Photocatalytic Wet Oxidation of Phenol

ARTICLE *in* THE JOURNAL OF PHYSICAL CHEMISTRY B · SEPTEMBER 2002

Impact Factor: 3.3 · DOI: 10.1021/jp025715y

Preparation of Nanosize Anatase and Rutile TiO_2 by Hydrothermal Treatment of Microemulsions and Their Activity for Photocatalytic Wet Oxidation of Phenol

Martin Andersson,*,† Lars Österlund,‡,§ Sten Ljungström,‡ and Anders Palmqvist†,‡

Department of Applied Surface Chemistry, Competence Centre for Catalysis, and Department of Applied Physics, Chalmers University of Technology, SE-412 96 Göteborg, Sweden

Received: March 4, 2002; In Final Form: June 14, 2002

Titanium dioxide (TiO_2) nanoparticles of both anatase and rutile phases were synthesized by hydrothermal treatment of microemulsions, and their photocatalytic activity for wet oxidation of phenol was studied. The only difference between the two syntheses used was that different acids were added to the microemulsions, making direct comparison of the catalytic activity of the two polymorphs possible. If hydrochloric acid was used, the rutile structure formed, and if nitric acid was used, anatase formed. The phase stability of the microemulsion was studied and according to conductivity and turbidity measurements the idea of a direct template effect could be discarded during the hydrothermal treatment. However, an initial size-templating phenomenon is possible during the mixing step. The particles, which were in the size range of a few nanometers were characterized with N_2-adsorption, XRD, SEM, and XPS. The activity of the two polymorphs for the photocatalytic oxidation of phenol in water was examined. It was shown that the rutile phase initially decomposed phenol much faster and follows a first-order process reasonably well ($k = 4 \times 10^{-5}$ s^{-1}). The photodecomposition process using the anatase phase led, however, to a much more rapid overall degradation following an initial slower rate of phenol oxidation. The results indicate that the observed difference of the photodecomposition process for the two TiO_2 phases is due to the formation of different intermediates.

1. Introduction

Photocatalytic degradation of organic compounds for the purpose of purifying water or wastewater from industries and households has under recent years gained a lot of attention.[1−4] Many of these organic substances are toxic and difficult to remove using traditional water cleaning facilities. The use of wide band gap semiconductors, especially titania, as photocatalysts to clean water is a very attractive method considering that the catalyst is nontoxic and of relatively low cost. The desired effect in this process is that photogenerated holes in the semiconducting titania oxidize the organic pollutant via intermediate products to CO_2 and water. Phenol is a widely used organic chemical present in a variety of wastewaters from various different industries, such as paper mills, textile industries, etc.[5−7] Phenol is quite toxic and slowly degradable in the environment, and it is hence of high environmental concern to find a good photocatalyst for its oxidation.[8,9]

Titania has previously been studied as a photocatalyst for the oxidation of phenol in both the anatase and the rutile forms.[10−14] From the previous studies it is not clear which of the two types is preferable because they are often present at the same time, as in the commercial DegussaP25, or they have not been prepared in a similar enough way to be comparable.[10−14] To our knowledge no work has been published when anatase and rutile have been compared for the photodegradation of phenol when they have both been produced with a hydrothermal synthesis method and at the same temperature. Several studies have been made comparing anatase and rutile prepared by different synthesis routes and at different temperatures. There are, however, many indications of catalytic differences depending on the way the titania has been prepared,[15] and studies where rutile has been prepared by heat treatment of anatase show results that are not consistent.[13,14]

In this work the titania particles were made using a microemulsion technique. A microemulsion is a thermodynamically stable, isotropic, and transparent mixture containing oil and water separated by a thin surfactant monolayer and can be either water in oil, oil in water, or bicontinuous.[16] In the present work water in oil microemulsions were used, and these consist of very small water droplets present in a pool of oil. The water droplets are typically in the size range of a few nanometers to 100 nm, and they can be used as small microreactors for chemical reactions.[17,18] By dissolving metal salts in the water pools followed by the addition of a reducing agent, researchers have prepared metals such as Cu, Pt, and Pd in the form of nanoparticles.[19−21] If instead two microemulsions containing salts of, e.g., $Cd(NO_3)_2$ and Na_2S are used, water insoluble compounds such as CdS can be prepared as nanoparticles.[22,23] The advantage with the microemulsion route is that the size of the particles can be affected by the ratio of surfactant to water. The sizes of the water droplets in the reverse microemulsions are approximately of the same size as the produced particles.[24] Mingmei Wu and co-workers showed that nanoparticles of both anatase and rutile type TiO_2 can be prepared at 120 °C by hydrothermal treatment of microemulsions.[25] Although their interpretation that the microemulsion templates the TiO_2 particle size at 120 °C is wrong (as will be shown in this communication), the outcome of their syntheses is of great interest because they yield the two titania polymorphs using the same temperature and the same synthesis method.

* Corresponding author. Tel: +46(0)31-7725611. Fax: +46(0)31-160062. E-mail: martina@surfchem.chalmers.se.
† Department of Applied Surface Chemistry.
‡ Competence Centre for Catalysis.
§ Department of Applied Physics.

10.1021/jp025715y CCC: $22.00
Published on Web 09/19/2002

TABLE 1: Compositions of Microemulsions Used for the Titania Syntheses

	component	volume
aqueous phase	tetrabutyl titanate	0.85 mL
aqueous phase	HCl (10 M) or HNO_3 (5 M)	1.0 mL of HCl or 2.0 mL of HNO_3
surfactant	TritonX-100	2.5 mL
cosurfactant	n-hexanol	1.5 mL
oil phase	cyclohexane	4 mL

2. Experimental Section

2.1. Starting Materials. TritonX-100 (*tert*-octylphenoxypolyethoxyethanol), 1-hexanol (98%, GC), cyclohexane (99%), titanium(IV) butoxide (97%), HCl (conc), HNO_3 (conc), and phenol (99%) were purchased from Aldrich and used as received. All water used was of milliQ grade.

2.2. Preparation of Titania. For the preparation of the reverse microemulsion system, TritonX-100 was used as the surfactant, *n*-hexanol as the cosurfactant, and cyclohexane as the continuous oil. Tetrabutyltitanate dissolved in either hydrochloric or nitric acid was used as the aqueous phase. The compositions used in the syntheses can be seen in Table 1. The titania syntheses were carried out according to the procedure described by Wu et al.[25] and was as follows. First a solution of surfactant, cosurfactant, and oil was prepared. Then the aqueous phase was added dropwise under stirring, making up the clear microemulsion. All the above steps were carried out at room temperature. The mixture was charged into a 45 mL Teflon-lined stainless steel autoclave. The autoclave was then heated to 120 °C and kept there for 13 h. After the hydrothermal treatment the precipitate found at the bottom of the autoclave was washed with ethanol several times to remove the oil, surfactant, and cosurfactant. The product was then kept in a desiccator to dry. No further heat treatment was done.

2.3. Characterization. X-ray diffraction patterns were recorded on the final products using a Siemens D5000 X-ray diffractometer and Cu Kα radiation of wavelength 1.54 Å in the range 20−60° (2θ). Scanning electron micrographs of the produced materials were obtained with a LEO 1525 FEG SEM and a Philips XL30 ESEM TMP. Nitrogen desorption isotherms were collected at 77 K using a Micromeritics ASAP 2010. Before the measurements the samples were exposed to vacuum treatment for 12 h at room temperature to remove any remaining moisture. The specific surface areas were obtained by the BET method,[26] and the pore size distributions were calculated from the N_2-desorption isotherm using the BJH method.[27] As-prepared titania samples were pressed into thin pellets using a manual hydraulic press (2 tonnes) and analyzed by XPS using a Perkin-Elmer PHI 5000C system with Mg Kα radiation (1253.6 eV). In addition to the survey spectra, high-resolution ($\Delta E = 0.025$ eV) spectra were collected for the Cl2p, N1s, and Ti2p and internally calibrated using the C1s peak as reference. The stability of the microemulsion was studied by conductivity and turbidity measurements using a Scanalys instrument[28] equipped with a LF 191 conductometer manufactured by WTW and a Hach Ratio XR turbidimeter manufactured by Hach Co. The phenol concentration was measured by UV absorption spectroscopy using a Shimadzu UV-160A spectrophotometer.

2.4. Photon-Irradiation Experiment. The optical setup used for the photon-irradiation experiments consisted of an arc lamp system (PTI) equipped with a 75 W Xe lamp and a 75 mm long water cell for filtering infrared radiation.[29] A set of lenses and apertures focused the light onto the open top-end of the continuously stirred batch photoreactor. The photoreactor consisted of an open glass beaker, which was wrapped in aluminum foil and water-cooled, keeping the irradiated liquid at a constant temperature of 9 °C. A volume of 16 mL of phenol/water solution with a phenol concentration of 0.001 wt % together with 29.5 mg of titania was transferred to the reactor, corresponding to 1.8 g/L of TiO_2. Samples of approximate 3 mL of the stirred slurry were taken at certain time intervals, keeping the titania/solution ratio constant. The slurry samples were then centrifuged in an ultracentrifuge at 15 000 rpm for 1 h to remove the titania. The clear solution was transferred to a 3 mL quartz cell with a beam length of 1 cm and analyzed with UV absorption. The amount of phenol was monitored by measuring the absorption at the wavelength of 271 nm. The absorption was converted to the phenol concentration referring to a standard curve showing a linear behavior between the concentration and the absorption at this wavelength. The light beam was in all experiments presented here directed through a cutoff filter (Oriel), which only transmitted photons in the UV region below 390 nm. However, to validate that only UV photons were active for the photocatalytic phenol decomposition process, control experiments were performed both with full arc illumination and with cutoff filers ($\lambda_{50\%} \sim 400$ nm) blocking the UV radiation. No photocatalytic effect was observed when the UV radiation was blocked. Similarly, photon irradiation of a sample containing no TiO_2 showed no changes in the phenol concentration upon photon irradiation. The photon irradiation was measured with a calibrated thermopile detector (Scientech) positioned in the same place as the photoreactor. The total power hitting the liquid surface was 120 mW. Although it is nontrivial to relate this quantity to a power density, we note that this corresponds roughly to a photon power density on the TiO_2 particles in the solution of 1.6 $\mu W/cm^2$ for anatase and 10.4 $\mu W/cm^2$ rutile, respectively, using the measured specific surface area of the different TiO_2 phases, and assuming that all photons hit the TiO_2 particles and that all particles are fully dispersed in the reactor. The total flux of UV photons, f_{UV}, impinging on the liquid surface was calculated from the known Xe lamp characteristics[29] (yielding the photon power per nm, P_λ) and the specified transmission of the cutoff filter, T_λ, and by integration over the UV wavelength region giving rise to significant photon transmission (200−390 nm), viz. $f_{UV} = \int P_\lambda T_\lambda \lambda/hc \, d\lambda$, yielding $f_{UV} = 1.9 \times 10^{17}$ photons/s. The total photon power, the estimated power density, and the photon flux were used to calculate the phenol decomposition probability and cross section, respectively.

3. Results and Discussion

3.1. Preparation and Characterization of Titanium Dioxide. In this work the focus was on comparing the activity for photodegradation of phenol over titanium dioxide of both rutile and anatase structure prepared at the same temperature by hydrothermal treatment of microemulsions. As has been shown earlier, the type of acid used in the synthesis has a major impact on which polymorph of titanium dioxide forms.[25] The microemulsion containing hydrochloric acid has a tendency to form the rutile structure of titania, whereas anatase is the structure obtained when nitric acid is used. From the XRD patterns shown in Figure 1 it can be seen that the two syntheses gave either anatase or rutile structures, and not a mixture of the two. From the diffraction patterns it is also obvious that the materials prepared are in the form of very small particles, as the peaks are very broad.

Using the Scanalys[28] equipment the phase boundaries of the microemulsions were studied. It was clear from the turbidity

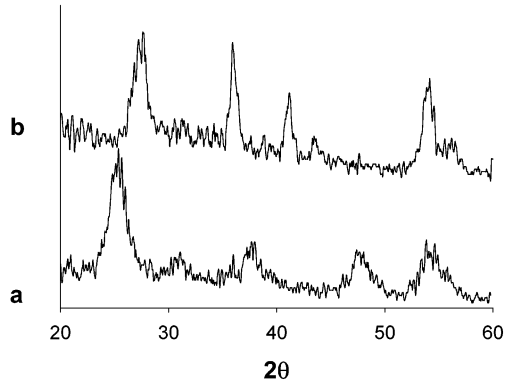

Figure 1. X-ray powder diffraction spectra of (a) anatase prepared from microemulsion containing HNO_3 and (b) rutile prepared from microemulsion containing HCl.

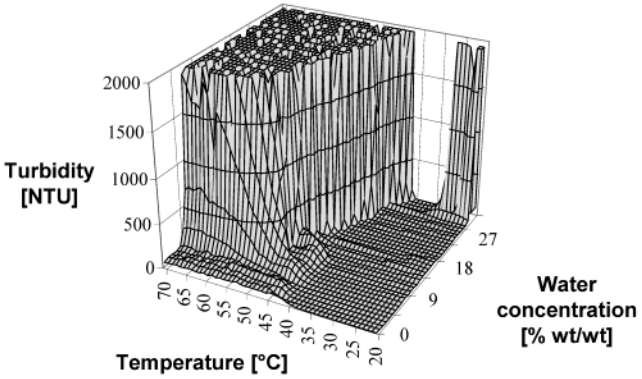

Figure 2. Turbidity of a solution containing 31.25% TritonX-100, 18.75% *n*-hexanol, and 50% cyclohexane vs temperature and water concentration obtained by Scanalys.

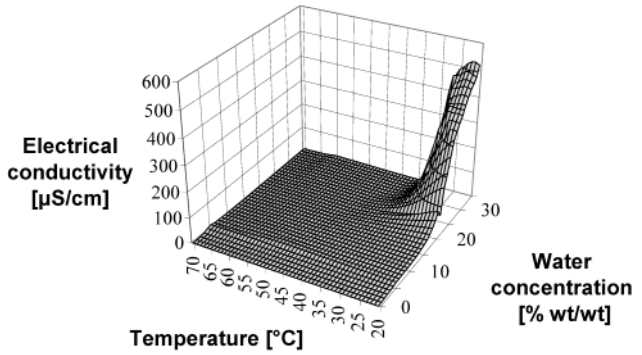

Figure 3. Electrical conductivity of a solution containing 31.25% TritonX-100, 18.75% *n*-hexanol, and 50% cyclohexane vs temperature and water concentration obtained by Scanalys.

measurement (Figure 2) that the turbidity was zero up to about 30% of added water and that the solution was clear up to about 40 °C. Figure 3 shows that the conductivity was low up to about 10% of water and very low at higher temperatures. From these data it is obvious that a microemulsion does not exist above 40 °C in this system. For this reason it is not possible that a droplet size templating effect was achieved at the hydrothermal conditions of 120 °C as previously suggested.[25] There is, however, a possibility that the droplet size templating effect was present during the mixing step of the preparation of the solution at room temperature. As the hydrolysis of the alkoxide is rapid in contact with water, it is possible that hydrolyzed particles of titania are formed at room temperature before the hydrothermal treatment. This would make the steps of the mixing and the aging of the reagent solution important variables of the synthesis.

The SEM micrographs in Figure 4 show a big difference in the morphology of the two crystalline structures. The anatase material consisted of agglomerated spherical particles of very narrow size distribution, whereas the rutile formed needle-shaped particles. This difference in morphology further supports the fact that there is no templating effect during the hydrothermal treatment. It is more likely that the different ions present during the synthesis (Cl^- or NO_3^-) influence the formation of the two different morphologies and crystal structures.[30] Figures 5 and 6 show the pore size distribution of the anatase and rutile samples, respectively. The narrow pore size distribution of the anatase material confirmed that the particles were monodisperse and packed in an ordered fashion. Both samples had their largest fraction of pore volume in the mesoporous region (30−50 Å), confirming that the particles were of a few nanometers in size. The ratio of the experimental value of the total pore volume of the pores in the anatase sample and the value taken from the calculations using the BJH method for the mesopores was 0.96. This showed that no micropores were present and that the high surface area of 256 m^2/g only came from the mesoporous region. For the rutile case, a not so well-defined pore size distribution was obtained and the specific surface area was 39 m^2/g. The explanation for this difference in surface area is believed to be that the rutile particles are needle-shaped instead of spherical and also larger in size. Because the two TiO_2 polymorphs were prepared in the presence of different anions (chloride or nitrate), XPS measurements were performed on the as-prepared rutile and anatase samples to investigate their presence on the surface. Figure 7 shows the XPS survey spectra and high-resolution (ΔE = 0.025 eV) spectra of the Ti2p, Cl2p, and N1s regions for the two samples. From these it can be seen that no significant difference exists in the surface chemical composition between the two samples. The XPS results show that the difference in the preparation procedure (the use of either HCl or HNO_3) does not result in any difference in the amount of adsorbed residues on the two titania surfaces.

3.2. Photodegradation of Phenol. The main reactions of the photocatalytic degradation of phenol have been suggested to be schematically represented by the following scheme:[10]

$$TiO_2 + h\nu \rightarrow TiO_2(h)^+ + e^- \quad (1)$$

$$TiO_2(h)^+ + H_2O(ads) \rightarrow {}^\bullet OH + H^+ + TiO_2 \quad (2)$$

$${}^\bullet OH + \text{phenol} \rightarrow \text{intermediate products (e.g., benzoquinone)} \quad (3)$$

$$TiO_2(h)^+ + \text{intermediate products} \rightarrow CO_2 + H_2O + TiO_2 \quad (4)$$

A UV photon ($h\nu$) creates an electron hole pair (1), which then reacts with water producing ${}^\bullet OH$ radicals as shown in reaction 2. This radical can further react with phenol, producing a whole range of intermediates such as benzoquinone (3). These products can then react with another ${}^\bullet OH$ radical or hole to finally produce carbon dioxide and water (4). The role of TiO_2 as a photocatalyst was verified in the present study by determining the wavelength dependence of the phenol decomposition process. Only UV photons with energy larger than the band gap energy of TiO_2 (ca. 3 eV, or $\lambda < 413$ nm) gave rise to a photocatalytic effect. The role of hydroxyl groups is also interesting in this context. Preliminary FTIR investigations on dried phenol-impregnated TiO_2 powders (anatase phase) indicate that the IR absorption in the OH-absorption region increases as a function of UV light exposure.

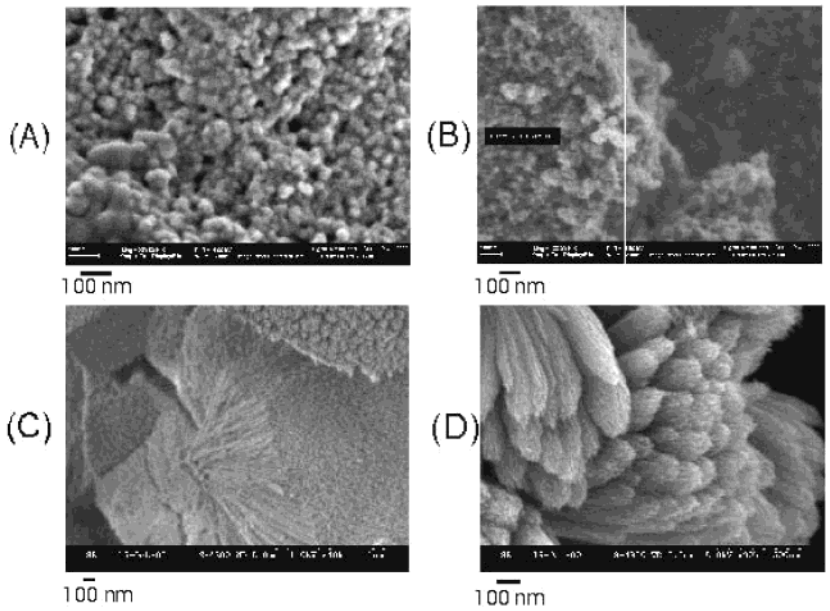

Figure 4. SEM micrographs of titania particles. (A) and (B) show anatase prepared from a microemulsion containing HNO_3; (C) and (D) show rutile prepared from a microemulsion containing HCl.

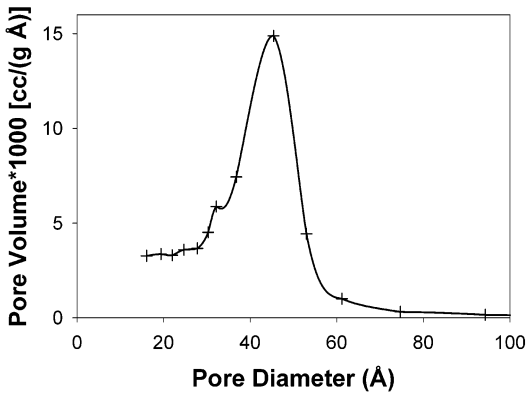

Figure 5. Pore size distribution of anatase determined from the N_2 adsorption isotherm using the BJH method.

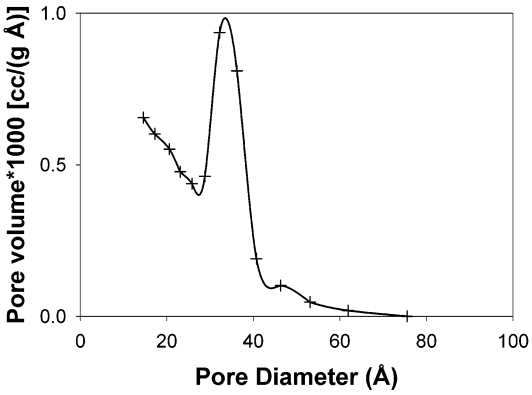

Figure 6. Pore size distribution of rutile determined from the N_2 desorption isotherm using the BJH method.

Parts a and b of Figure 8 show the absorption spectra of the centrifuged slurry samples taken from the photocatalytic reactor after various times of UV exposure, for the anatase and rutile samples, respectively. The graphs were adjusted so that the point at 300 nm was at zero absorbance. This was done because small amounts of titania were always present, raising the background at this wavelength. Experiments with known phenol concentrations with different amounts of added titania were tested to justify this procedure. The phenol peak at 271 nm is in Figure 9 plotted as a function of duration of UV exposure, and also as a function of the total photon flux. From these curves it is evident that a higher initial rate of degradation of phenol occurred for the sample containing the rutile phase, whereas the anatase sample became more effective after more than 3 h of UV exposure. It is also seen that the types of the phenol decomposition processes are different for the anatase and the rutile samples, respectively. The decomposition process for the rutile sample can be reasonably well described by a first-order process with a rate constant of ca. 4×10^{-5} s^{-1} (dotted line in Figure 9). This corresponds to an overall photodecomposition probability for UV photons ($\lambda <$ 390 nm) of 2.1×10^{-22} per photon or cross section of $\sigma \approx 2.4 \times 10^{-18}$ cm^2 using the estimated power density on the rutile sample. The decomposition process on the anatase sample cannot be described by simple kinetics. First, the data show an initial "induction" period, where the phenol decomposition rate is slow. After irradiation for more than 3 h, or equivalently after a total photon flux into the sample compartment of $>2 \times 10^{21}$ photons, the decomposition became very rapid; in fact, much more rapid than a simple first-order process. This difference in degradation kinetics between rutile and anatase is believed to be due to two different degradation mechanisms of phenol, where different intermediates are formed. The absorption spectra in Figure 8 show a peak around 245 nm, which only appears for the anatase case. This peak is plotted as a function of time and UV exposure in Figure 10 and is believed to come from benzoquinone, which is one of the many different intermediates that have been reported to form during the degradation.[10] Another observed difference between the two catalysts is that during the irradiation the anatase powder changed its color to a more brownish one, but after a longer time of irradiation the color disappeared. This is consistent with the absorption at 245 nm, which shows that the benzoquinone has a maximum concentration at the same time of irradiation at which the powder has its brownish color. No visible color changes were, however, observed for the rutile-containing sample, also consistent with the absorbance spectrum, showing a low and constant absorbance value for the rutile catalyst in the UV−vis.

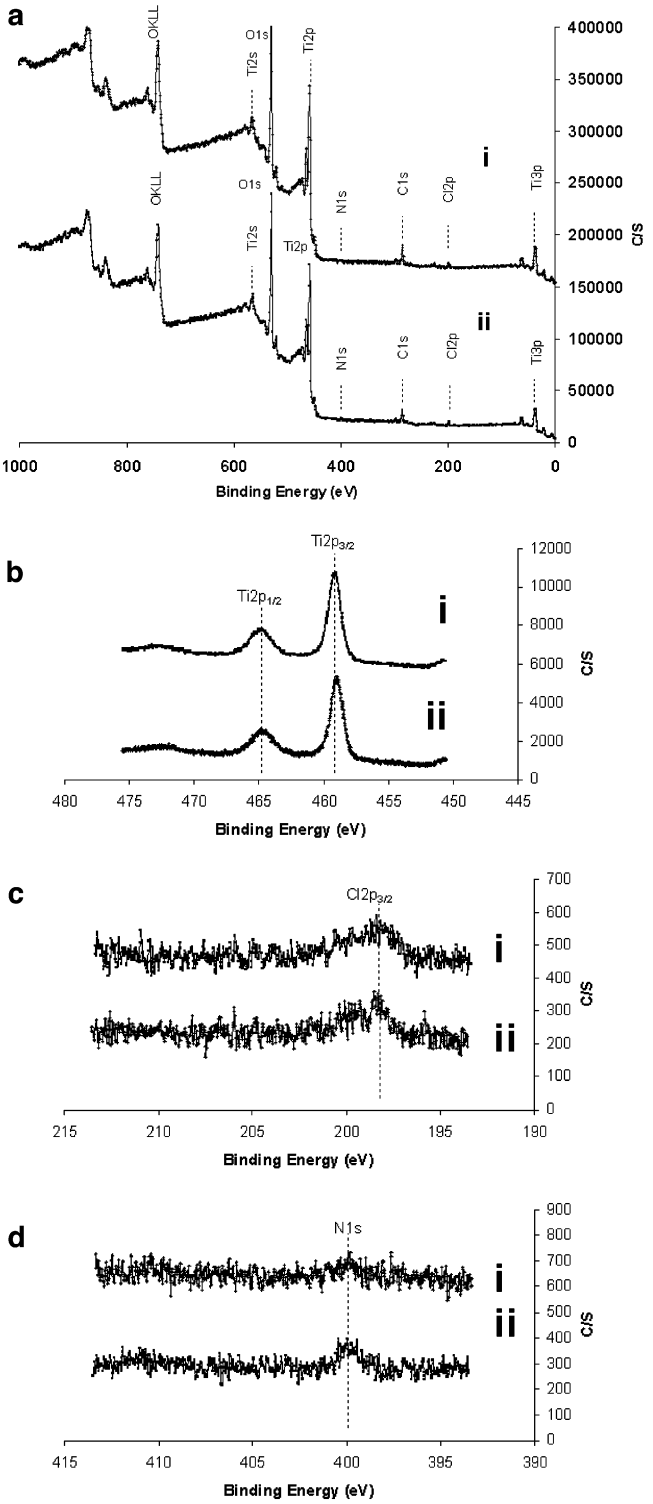

Figure 7. XPS analysis of the as-prepared anatase (i) and rutile (ii) samples showing (a) the survey spectra and (b) the Ti2p, (c) the Cl2p, and (d) the N1s high-resolution regions internally calibrated using the C1s peak as reference.

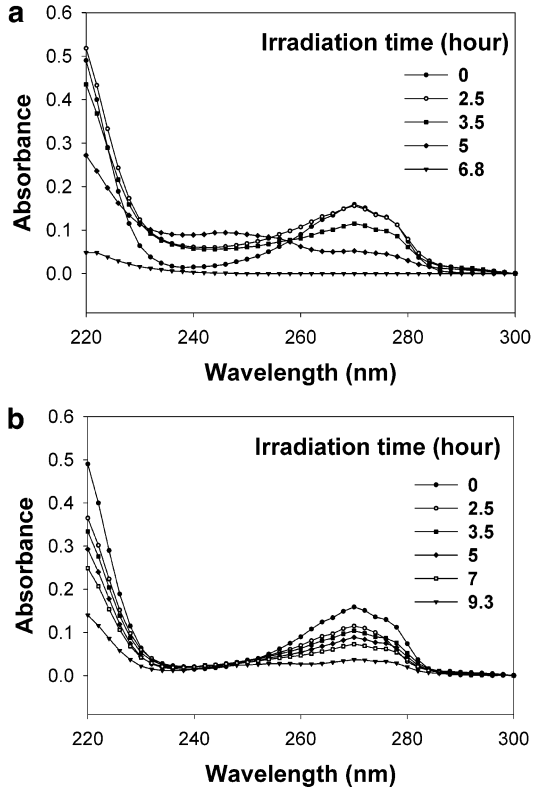

Figure 8. Absorbance of centrifuged samples taken from the photocatalytic reactor after various times of UV exposure vs wavelength for (a) anatase and (b) rutile samples. The graphs are adjusted so that the point at 300 nm was at zero absorbance.

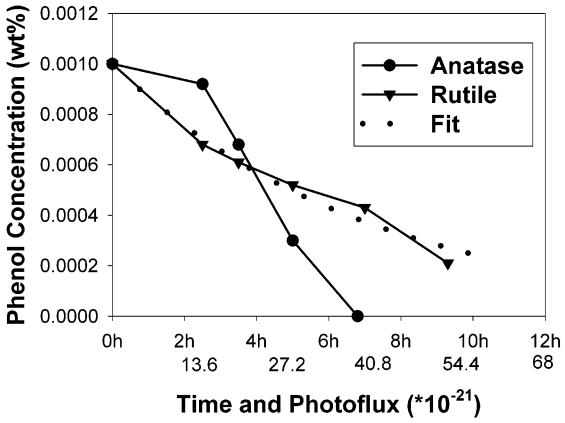

Figure 9. Phenol concentration plotted as a function of time of UV exposure and of the total photoflux hitting the reaction mixture for both anatase and rutile together with a fit for the rutile case (dotted). The fit follows a first-order process with a rate constant of ca. 4×10^{-5} s^{-1}.

4. Conclusions

Nanosized titania was synthesized using the method of hydrothermal treatment of microemulsions. When the microemulsion contained hydrochloric acid, the rutile structure formed, whereas the anatase was obtained when nitric acid was used. The syntheses were all made at 120 °C, and no further heat treatment was applied. It was found from the turbidity and conductivity measurements that the microemulsion cannot work as a template during the hydrothermal treatment but could work as an initial size template during the mixing step.

The photocatalytic activity for the photodegradation of phenol was compared for the two titania polymorphs. From this study, the following conclusions can be drawn: (1) Both anatase and rutile are active in the photocatalytic reaction, but a difference in the kinetics could be observed. The rutile gave a faster initial degradation of phenol, whereas anatase led to a much faster total degradation after an initial slower rate. (2) Different intermediates were formed during the reaction, indicating different decomposition mechanisms for rutile compared to anatase. This was observed both as an appearing absorbance peak at 241 nm and as a color change on the titania for the

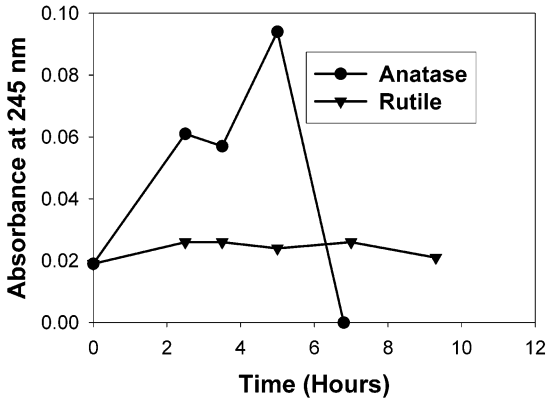

Figure 10. Absorbance at 245 nm plotted as a function of UV exposure. The peak for the anatase case after 5 h is believed to come from benzoquinonone, which is one of many intermediates that have been observed during degradation of phenol.

anatase case. None of these observations could be seen for the rutile powder.

Acknowledgment. We acknowledge the Foundation of Strategic Research through its Colloid and Interface Technology program for financial support. We thank the Competence Centre for Catalysis, which is financially supported by the Swedish National Energy Administration and the member companies: AB Volvo, Johnson Matthey CSD, Saab Automobile AB, Perstorp AB, Eka Chemicals AB, MTC AB, and Swedish Space Corp. We also thank Dr. Zhongxi Sun for the Scanalys measurements.

References and Notes

(1) Ollis, D. F.; Al-Ekabi, H. *Photocatalytic Purification and Treatment of Water and Air*; Elsevier: Amsterdam, 1993.
(2) Hoffman, M. R.; Martin, S. T.; Choi, W.; Bahnemann, D. W. *Chem. Rev.* **1995**, *95*, 69.
(3) Serpone, N.; Maruthamuthu, P.; Pichat, P.; Pelizzetti, E.; Hidaka, H. *J. Photochem. Photobiol. A* **1995**, *85*, 247.
(4) Baird, C. *Environmental Chemistry*; Freeman: New York, 1998; p 330.
(5) Hachem, C.; Bocquillon, F.; Zahraa, O.; Bouchy, M. *Dyes. Pigments* **2001**, *49*, 117.
(6) Yeber, M. C.; Rodriguez, J.; Baeza, J.; Durán, N.; Mansilla, H. D. *Chemosphere* **1999**, *39*, 1679.
(7) Balcioglu, L. A.; Arslan, I. *Environ. Pollution* **1998**, *103*, 261.
(8) Saha, N. C.; Bhunia, F.; Kaviraj, A. *Bull. Environ. Contam. Toxicol.* **1999**, *63*, 195.
(9) Tisler, T.; Zagorc-Koncan, J. *Water. Air. Soil. Pollution* **1997**, *97*, 3−4, 315.
(10) Pieró, A. M.; Ayllón, J. A.; Peral, J.; Doménech, X. *Appl. Catal. B Environ.* **2001**, *30*, 359.
(11) Chen, D.; Ray, A. K. *Appl. Catal. B Environ.* **1999**, *23*, 143.
(12) Tsai, S.; Cheng, S. *Catal. Today* **1997**, *33*, 227.
(13) Chhabra, C.; Pillai, V.; Mishra, B. K.; Morrone, A.; Shah, D. O. *Langmuir* **1995**, *11*, 3307.
(14) Ding, Z.; Lu, G. O.; Greenfield, P. F. *J. Phys. Chem. B* **2000**, *104*, 4815.
(15) Sclafani, A.; Palmisano, L.; Schiavello, M. *J. Phys. Chem.* **1990**, *94*, 829.
(16) Kumar, P.; Mittal, K. L. *Handbook of Microemulsion Science and Technology*; Mercel Dekker: New York, 1999.
(17) Pillai, V.; Kumar, P.; Hou, M. J.; Ayyub, P.; Shah, D. O. *Adv. Colloid Interface Sci.* **1995**, *55*, 241.
(18) Pileni, M. P. *J. Phys. Chem. B* **1993**, *97*, 6961.
(19) Chen, D. H.; Yeh, J. J.; Huang, T. C. *J. Colloid Interface Sci.* **1999**, *215*, 159.
(20) Qi, J.; Ma, J.; Shen, J. *J. Colloid Interface Sci.* **1997**, *186*, 498.
(21) Shen, D. H.; Wang, C. C.; Huang, T. D. *J. Colloid Interface Sci.* **1999**, *210*, 123.
(22) Curri, M. L. *J. Phys. Chem. B* **2000**, *104*, 8391.
(23) Agostiano, A.; Catalano, M.; Curri, M. L.; Della Monica, M.; Manna, L.; Vasanelli, L. *Micron* **2000**, *31*, 253.
(24) Pileni, M. P. *Langmuir* **1997**, *13*, 3266.
(25) Wu, M.; Long, J.; Huang, A.; Luo, Y. *Langmuir* **1999**, *15*, 8822.
(26) Brunauer, S.; Emmett, P. H.; Teller, E. *J. Am. Chem. Soc.* **1938**, *60*, 309.
(27) Barret, E. P.; Joyner, L. G.; Halenda, P. P. *J. Am. Chem. Soc.* **1951**, *73*, 373.
(28) Sun, Z.; Sköld, R. O. *J. Colloid Interface Sci.* **2001**, *242*, 67.
(29) Hellsing, B. *J. Chem. Phys.* **1997**, *106*, 982.
(30) Matijevic, E. *J. Colloid Interface Sci.* **1977**, *58*, 374.